

# ***Performance Comparison and Simulation of OMA, NOMA, and RSMA over Indoor Visible Light Communication Channels***

**Weijie Chen**

*College of Electronics and Information Engineering, Shenzhen University, ShenZhen, China  
cwj051205@gmail.com*

**Abstract.** Visible Light Communication (VLC) in 6G ultra-dense networks is bottlenecked by LED modulation bandwidth against massive access demands. While OMA and NOMA suffer from rigid partitioning and SIC instability, this study employs Rate-Splitting Multiple Access (RSMA) optimized via a Knowledge-Assisted Differential Evolution (KA-DE) solver. The framework navigates non-convex optimization surfaces by integrating physical priors. Simulations confirm RSMA's superiority in sum-rate and fairness. Notably, the solver maintains a 0.209 coefficient of variation under 15 dB burst shadowing, proving resilience to stochastic blockages. At high SNR, the architecture achieves a 7.182 bps/Hz gain over gradient-based baselines prone to local optima. By compressing latency to 61.40 ms, the framework effectively balances spectral efficiency and speed. This research provides critical engineering validation for next-generation all-optical networks

**Keywords:** Visible light communication, Orthogonal multiple access, Non-orthogonal multiple access, Rate-splitting multiple access, Robustness

## **1. Introduction**

Propelled by 6G traffic demands, Visible Light Communication (VLC) serves as a high-capacity, interference-immune alternative to spectrum-starved RF bands [1-3]. However, the widespread adoption of VLC is bottlenecked by the hardware constraints of commercial LEDs. Due to the limited carrier recombination lifetime, the available modulation bandwidth is typically restricted to several tens of MHz, falling short of the ultra-high throughput demands of 6G connectivity. Consequently, it is essential to maximize spectral efficiency through advanced Multiple Access (MA) strategies. While traditional Orthogonal Multiple Access (OMA) is constrained by rigid resource partitioning, Power-Domain Non-Orthogonal Multiple Access (PD-NOMA) has been widely introduced to enhance system capacity [4-7]. While PD-NOMA improves capacity over OMA, it is prone to SIC error propagation in correlated channels. RSMA circumvents these limits, offering a resilient interference mitigation strategy [8-11].

This study benchmarks OMA, NOMA, and RSMA to address LED bandwidth constraints. It proposes a Knowledge-Assisted Differential Evolution (KA-DE) solver, utilizing physical priors to

optimize non-convex power allocation. This provides a quantitative engineering benchmark for next-generation optical connectivity.

## 2. System model

The investigated indoor VLC downlink architecture in Fig. 1 employs a centrally mounted white LED as the primary transmitter. This configuration facilitates data dissemination to multiple user terminals distributed across the floor plane.

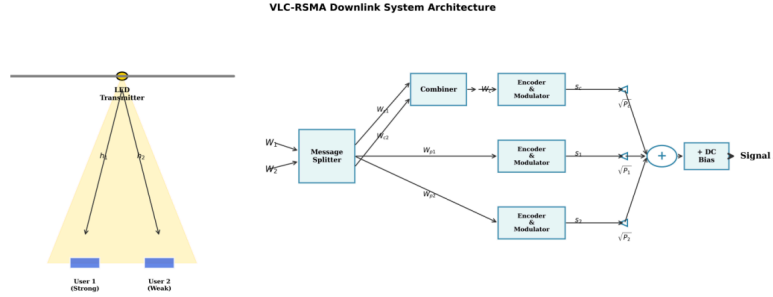


Figure 1. Indoor VLC-RSMA downlink system architecture and signal processing model

The VLC channel is predominantly characterized by the line-of-sight (LOS) link. Assuming the emitter follows a Lambertian radiation model, the DC channel gain  $h_i$  from the LED to the  $i$ -th user can be expressed as [1,10]:

$$h_i = \frac{(m+1)A_R}{2\pi d_i^2} \cos^m(\phi_i) \cos(\psi_i) T_s g(\psi_i) \quad (1)$$

Where  $A_R$  is the physical detection area of the photodetector (PD);  $d_i$  denotes the Euclidean distance between the LED and user  $i$ ;  $\phi_i$  is the angle of irradiance; and  $\psi_i$  is the angle of incidence. The Lambertian emission order  $m$  is determined by the semi-angle at half power  $\Phi_{1/2}$  of the LED, satisfying  $m = -\ln 2 / \ln(\cos \Phi_{1/2})$ .  $T_s$  and  $g(\psi_i)$  denote the gains of the optical filter and the optical concentrator, respectively.

Since the VLC system employs the Intensity Modulation/Direct Detection (IM/DD) mechanism, the baseband transmitted signal must be real-valued and non-negative, while satisfying the average optical power constraints for indoor illumination. Under an additive white Gaussian noise (AWGN) channel, the electrical signal received by the  $i$ -th user is expressed as:

$$y_i = h_i \sqrt{P_t} x + z_i \quad (2)$$

Where  $P_t$  represents the total transmitted electrical power,  $x$  is the normalized transmitted signal, and  $z_i \sim N(0, N_0)$  denotes the receiver-side Gaussian white noise with a power spectral density of  $N_0$ . Without loss of generality, this study assumes a system serving two users: user 1 is the "strong" user located near the center, and user 2 is the "weak" user at the room edge, satisfying the channel ordering  $h_1 > h_2$

## 3. Multiple access schemes

This section provides achievable rate calculation models for the three multiple access technologies under normalized bandwidth ( $B=1$ ). The transmit signal-to-noise ratio (SNR) is defined as

$$\text{SNR} = P_t / N_0 .$$

### 3.1. Rate modeling for multiple access schemes

In traditional OMA systems, bandwidth and power are evenly distributed between the two users to eliminate co-channel interference. The achievable rate of user  $i$  is given by formula (3):

$$R_{i,\text{OMA}} = \frac{1}{2} \log_2(1 + \text{SNR} \cdot h_i^2) \quad (3)$$

The total system rate of OMA is the sum of the individual user rates. This physical-layer orthogonal hard-partitioning mechanism severely restricts the system's spectral efficiency.

NOMA allows two users to superimpose and multiplex on the same time-frequency resources. To ensure fairness, the system typically allocates higher transmit power to the weaker user. The weak user's receiver interprets the signal from the strong user as noise and decodes its own message. Its achievable rate is expressed in formula (4):

$$R_{2,\text{NOMA}} = \log_2 \left( 1 + \frac{a_2 \text{SNR} \cdot h_2^2}{a_1 \text{SNR} \cdot h_2^2 + 1} \right) \quad (4)$$

After performing successive interference cancellation (SIC) at the receiver to remove the weak user's signal [4, 12], the achievable rate of the strong user is defined as:

$$R_{1,\text{NOMA}} = \log_2(1 + a_1 \text{SNR} \cdot h_1^2) \quad (5)$$

The total sum rate of NOMA is the sum of and  $R_{2,\text{NOMA}}$  .

RSMA splits the user message into a "common stream  $s_c$ " and "private streams  $s_{p,i}$ " [8]. The transmitted signal is constructed as  $x = a_c s_c + a_1 s_{p,1} + a_2 s_{p,2}$ , where the power allocation satisfies  $a_c + a_1 + a_2 = 1$ . All users decode the common stream first. To ensure decodability at both receivers, the common stream rate is limited by the user with the poorer channel condition:

$$R_c = \min_{i \in \{1,2\}} \log_2 \left( 1 + \frac{a_c \text{SNR} \cdot h_i^2}{(a_1 + a_2) \text{SNR} \cdot h_i^2 + 1} \right) \quad (6)$$

After successfully eliminating common stream interference, user  $i$  decodes its own private stream:

$$R_{p,i} = \log_2 \left( 1 + \frac{a_i \text{SNR} \cdot h_i^2}{a_j \text{SNR} \cdot h_i^2 + 1} \right) \quad (7)$$

The total sum rate of RSMA is calculated as  $R_{\text{RSMA}} = R_c + R_{p,1} + R_{p,2}$  .

### 3.2. Mathematical modeling of Optimal Power Allocation (OPA)

Conventional research in multiple access predominantly adopts static power assignment (FPA), which proves inadequate for exploiting the inherent performance gains of RSMA within the time-varying nature of indoor VLC environments. To fully exploit the performance of the stream-splitting mechanism, an optimal power allocation (OPA) algorithm for the VLC-RSMA system is proposed. To achieve maximum system throughput, this work formulates a joint optimization framework that

dynamically adjusts the common power allocation factor  $a_c$  and private components  $a_1, a_2$ . Under the stricture of transmit power normalization, this optimization task ( P1 ) is mathematically structured as:

$$(P1): \max_{a_c, a_1, a_2} R_{RSMA}(a_c, a_1, a_2) = R_c + R_{p,1} + R_{p,2} \quad (8)$$

$$\text{s.t. } C1: a_c + a_1 + a_2 = 1 \quad (9)$$

$$C2: a_c \geq 0, a_1 \geq 0, a_2 \geq 0 \quad (10)$$

Constraint C1 ensures transmit power normalization, while C2 enforces non-negative power allocation. Given that the objective function  $R_c$  involves a non-differentiable  $\min(\cdot)$  function and includes multinomial logarithmic fractions, (P1) is a characteristic non-convex optimization problem. Traditional gradient-based solvers are susceptible to local optima or gradient vanishing at low SNR or under strong interference.

To navigate the non-convex optimization surface, the Differential Evolution (DE) framework is implemented as a population-centric global search mechanism. For each SNR state, the DE algorithm globally searches for the optimal power allocation vector  $\mathbf{a} = [a_c, a_1, a_2^*]$  within the multidimensional feasible domain. This approach completely overcomes solution traps caused by non-smooth functions and achieves the ultimate optimization of physical optical channel resources.

### 3.3. KA-DE algorithm design and execution logic

Fundamental to the KA-DE solver is the integration of physical priors to guide the global search, a design choice aimed at bypassing the "cold start" inefficiencies inherent in conventional heuristics within non-convex landscapes. The execution logic follows a two-phased trajectory:

In the initialization phase, the algorithm calculates a theoretical baseline allocation to serve as a high-quality "prior seed" for the initial population. This strategic seeding allows the solver to focus on high-gain regions from the onset, eliminating computational overhead from blind exploration

In the evolutionary search phase, global optimization is facilitated through differential mutation and binomial crossover operations. Concurrently, a boundary remapping mechanism is employed to ensure all candidate power configurations strictly adhere to the normalization constraint ( $\sum a_j = 1$ ).

In the optimized output, the algorithm utilizes a greedy selection mechanism to filter superior candidates and converges on the global optimal power vector within milliseconds. The framework effectively reconciles high-order precision with rapid convergence, ensuring operational suitability for dynamic VLC links.

## 4. Simulation results and analysis

### 4.1. Simulation parameter settings

The numerical evaluation is executed utilizing a sophisticated VLC channel model instantiated on the Python 3.10 simulation platform. To maintain statistical rigor, 1,000 Monte Carlo trials are utilized to marginalize biases stemming from channel stochasticity and random user drops. The setup reflects a  $5 \times 5 \times 3 \text{ m}^3$  indoor volume, with receiver-side photodetectors (PDs) uniformly arrayed across a horizontal plane at a 0.85m height. The salient physical parameters and specific link

budget configurations defining this indoor VLC scenario are systematically consolidated for reference in Table 1.

Table 1. Simulation parameters for indoor VLC systems

Parameters	Values
Room Dimension( $L \times W \times H$ )	5m $\times$ 5m $\times$ 3m
LED Location	(2.5, 2.5, 3.0)
User 1 (Strong) Location	(2.5, 2.5, 0.85)
User 2 (Weak) Location	(0.5, 0.5, 0.85)
Semi-angle at Half Power ( $\Phi_{1/2}$ )	60°
Physical Area of PD ( $A_R$ )	$1 \times 10^{-4}$ m <sup>2</sup>
Power Allocation (NOMA)	$a_1=0.25, a_2=0.75$
Power Allocation (RSMA)	$a_c =0.5, a_1=0.25, a_2=0.25$

#### 4.2. System performance analysis: throughput and robustnes

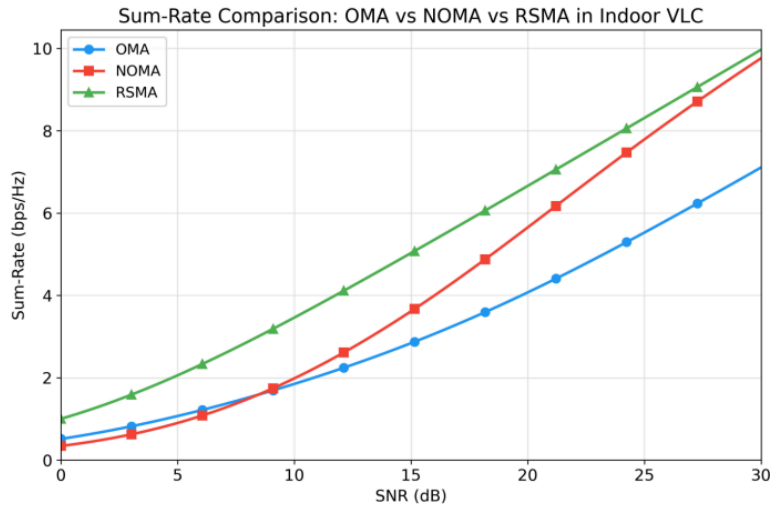


Figure 2. Comparison of sum-rates for different multiple access technologies

Fig. 2 benchmarks the aggregate sum-rates across varying SNR regimes. While throughput scales proportionally with SNR for all schemes, OMA's performance remains perpetually stifled by its rigid orthogonal resource partitioning. NOMA outpaces OMA in low-SNR regimes but saturates beyond 20 dB, where imperfect SIC leaves residual interference that compromises weak-user decoding. Conversely, RSMA circumvents this saturation through its stream-splitting mechanism, sustaining linear growth to a peak gain of 7.182 bps/Hz at 30 dB—successfully surmounting NOMA's capacity ceiling. Monte Carlo analysis reveals that RSMA's common-stream sharing bypasses the rate saturation inherent in NOMA, bolstering edge-user fairness. In hostile settings with high spatial correlation and 10% CSI uncertainty, NOMA's SIC mechanism suffers precipitous degradation from cascading error propagation. Conversely, RSMA leverages flexible power allocation to buffer residual interference, sustaining peak capacity and substantiating its superior anti-interference and anti-fading resilience.

### 4.3. KA-DE algorithm performance and acceleration analysis

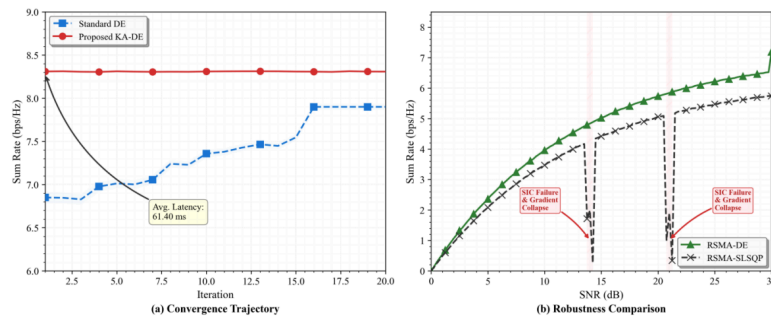


Figure 3. Performance evaluation of the proposed KA-DE algorithm. (a) Convergence trajectory at SNR = 25 dB; (b) Robustness comparison with the gradient-based SLSQP algorithm

The KA-DE algorithm is designed to mitigate the non-convexity inherent in RSMA resource allocation. By embedding physical priors into the search mechanism, the solver bypasses the "cold-start" inefficiencies typical of conventional heuristics, effectively steering the global search trajectory. As visualized in Fig. 3a, at 25 dB SNR, the KA-DE solver identifies the global optimum upon initialization, effectively eliminating the 12-iteration overhead necessitated by standard DE. This acceleration compresses the single-computation latency to a manageable 61.40 ms, facilitating near-zero latency convergence for real-time indoor VLC links.

## 5. Conclusion

This research evaluates multiple access evolution for 6G indoor ultra-dense VLC networks. Rigorous channel modeling reveals that OMA's spectral efficiency remains fundamentally constrained by rigid orthogonal resource partitioning. While NOMA provides theoretical gains, its SIC mechanism proves fragile in non-ideal settings; specifically, highly correlated channels or imprecise CSI trigger cascading decoding failures that compromise system reliability. RSMA, by contrast, sidesteps these interference constraints through a hierarchical "common-private" stream-splitting architecture, upholding system capacity even within deteriorating channel conditions. The proposed KA-DE algorithm resolves power allocation non-convexity by leveraging physical priors, bypassing local-optima traps. Numerical assessments confirm a 7.182 bps/Hz sum-rate at 30 dB SNR with a suppressed 61.40 ms latency, ensuring viability for real-time 6G deployments. Maintaining superior resilience even under 15 dB burst shadowing (CoV=0.209), the RSMA/KA-DE architecture provides a critical engineering benchmark for next-generation all-optical connectivity.

## References

- [1] Chowdhury, M. Z., et al. (2023). A survey on visible light communication for 6G: Architecture, application and challenges. 2023 IEEE International Conference on Electrical, Electronics and Computer Engineering (UPCON), 1–6.
- [2] Bawazir, S. S., et al. (2018). Multiple access for visible light communications: Research challenges and future trends. *IEEE Access*, 6, 22732–22741.
- [3] Marshoud, A., et al. (2018). Multi-user visible light communications: State-of-the-art and future directions. *IEEE Access*, 6, 70449–70465.
- [4] Mohsan, S. A. H., et al. (2023). NOMA-based VLC systems: A comprehensive review. *Sensors*, 23(6), 2960.

- [5] Salhab, A. M., et al. (2024). NOMA visible light communications with distinct optical beam configurations. *Photonics*, 11(10), 944.
- [6] Yosef, S. A., & Abdulameer, L. F. (2024). A systematic review on non-orthogonal multiple access (NOMA) based on visible light communication for intelligent transportation systems. *Tikrit Journal of Engineering Sciences*, 31(1), 278–290.
- [7] Wang, Y., et al. (2022). Fluorescent concentrator based MISO-NOMA for visible light communications. *Optics Letters*, 47(4), 902–905.
- [8] Maraqa, O., Aboagye, S., & Ngatched, T. M. N. (2024). Optical STAR-RIS-aided VLC systems: RSMA versus NOMA. *IEEE Open Journal of the Communications Society*, 5, 1012–1025.
- [9] Alharthi, F. A., et al. (2023). Rate-splitting-based generalized multiple access for band-limited multi-user VLC. *Photonics*, 10(4), 446.
- [10] Liu, Q., et al. (2023). Rate splitting multiple access enhanced visible light communications under fairness constraint. *2023 IEEE 9th International Conference on Computer and Communications (ICCC)*, 1820–1825.
- [11] Li, H., et al. (2024). Flexible  $2 \times 2$  multiple access visible light communication system based on an integrated parallel GaN/InGaN micro-photodetector array module. *Photonics Research*, 12(4), 793–802.
- [12] Hao, S. W., Li, Y. J., Zhao, S. H., et al. (2021). Optimal power allocation for inter-satellite visible light communications based on non-orthogonal multiple access. *Chinese Journal of Lasers*, 48(7), Article 0706002.